HHS Public Access

Author manuscript

Clin Cancer Res. Author manuscript; available in PMC 2019 January 01.

Published in final edited form as:

Clin Cancer Res. 2018 January 01; 24(1): 62–72. doi:10.1158/1078-0432.CCR-17-0357.

Phase Ib Study of Immune Biomarker Modulation with Neoadjuvant Cetuximab and TLR8 stimulation in Head and Neck Cancer to Overcome Suppressive Myeloid Signals

Gulidanna Shayan[1], **Benjamin A. Kansy**[2], **Sandra P. Gibson**[4], **Raghvendra M. Srivastava**[3], **James Kyle Bryan**[5], **Julie E. Bauman**[4], **James Ohr**[4], **Seungwon Kim**[4], **Umamaheswar Duvvuri**[4], **David A. Clump**[4], **Dwight E. Heron**[4], **Jonas T. Johnson**[4], **Robert M. Hershberg**[5], and **Robert L. Ferris**[3]

[1]School of Medicine, Tsinghua University, Beijing, China

[2]Department of Otolaryngology University Hospital Essen, Germany

[3]Department of Otolaryngology, University of Pittsburgh, Pittsburgh, PA, USA

[4]University of Pittsburgh Cancer Institute, Pittsburgh, PA, USA

[5]VentiRx Pharmaceuticals Inc., Seattle, WA, USA

Abstract

Purpose—The response rate of head and neck squamous cell carcinoma (HNSCC) patients to cetuximab therapy is only 15–20%, despite frequent EGFR overexpression. Since immunosuppression is common in HNSCC, we hypothesized that adding a pro-inflammatory TLR8 agonist to cetuximab therapy might result in enhanced T lymphocyte stimulation and anti-EGFR specific priming.

Experimental Design—Fourteen patients with previously untreated HNSCC were enrolled in this neoadjuvant trial and treated preoperatively with 3–4 weekly doses of motolimod (2.5 mg/m^2) and cetuximab. Correlative tumor and peripheral blood specimens were obtained at baseline and at the time of surgical resection and analyzed for immune biomarker changes. Preclinical *in vitro* studies were also performed to assess the effect of cetuximab plus motolimod on myeloid cells.

Results—TLR8 stimulation skewed monocytes toward an M1 phenotype and reversed MDSC suppression of T cell proliferation *in vitro*. These data were validated in a prospective phase Ib neoadjuvant trial, in which fewer MDSC and increased M1 monocyte infiltration were found in TIL. Motolimod plus cetuximab also decreased induction of Treg, and reduced markers of suppression, including CTLA-4, CD73 and membrane bound TGF-β. Significantly increased circulating EGFR-specific T cells were observed, concomitant with enhanced CD8+ T cell infiltration into tumors. These T cells manifested increased TCR clonality, upregulation of the costimulatory receptor CD27, and downregulation of inhibitory receptor TIGIT.

Correspondence: Robert L. Ferris, MD, PhD, Hillman Cancer Center Research Pavilion, 5117 Centre Avenue, Room 2.26b, Pittsburgh, PA 15213-1863, Phone: 412-623-0327, ferrrl@upmc.edu.

Conflicts of Interest statement: Robert L. Ferris: consulting or advisory role: AstraZeneca, Bristol-Myers Squibb, Merck, ONO Pharmaceutical and Celgene. Research funding: Amgen (Inst), Bristol-Myers Squibb (Inst.) AstraZeneca (Inst.) and VentiRx (Inst.). Robert M. Hershberg is an employee of VentiRx and Celgene Inc. James Kyle Bryan is an employee of VentiRx.

Conclusion—Enhanced inflammatory stimulation in the tumor microenvironment using a TLR agonist overcomes suppressive myeloid and regulatory cells, enhancing the cellular antitumor immune response by therapeutic mAb in HNSCC.

Keywords

head and neck cancer; cetuximab; TLR8; monoclonal antibody; immunotherapy

Introduction

Head and neck squamous cell carcinoma (HNSCC) is the sixth leading cancer by incidence worldwide, with a 5-year survival rate of around 40–50% despite recent advances in surgery, chemotherapy and radiotherapy (1–3). As HNSCC has a high prevalence of epidermal growth factor receptor (EGFR) overexpression (80–90%), anti-EGFR monoclonal antibodies (mAbs) remain an important targeted therapy for treatment of the disease (3, 4). In addition to blocking EGFR-mediated growth signals in tumor cells, cetuximab can also mediate antibody-dependent cell-mediated cytotoxicity (ADCC) (5) and facilitate cross-talk between NK cells and dendritic cells (DC), which in turn may induce expansion of EGFR-specific cytotoxic T lymphocytes (CTL) (6, 7). However, the response rate to cetuximab therapy in HNSCC patients is only about 15–20% (8). Our recent findings suggest that suppressive immune cells contribute to this poor prognosis (9) and demonstrate the potential to improve clinical outcome by reversing the suppressive tumor microenvironment (TME).

Given the impact of innate immune cells on clinical response to immunotherapy (10), the antitumor properties of molecules targeting the innate immune system are an emerging area of interest (11). For instance, myeloid derived antigen presenting cells (APC) have been shown to play an essential role in shaping the TME, engaging in antitumor functions as well as the enhancement of tumor progression (12, 13). Their activity can be modulated by Toll-like receptors (TLR), pro-inflammatory innate pattern recognition receptors that induce NF-kB dependent signaling and release of cytokines, which promote antitumor immunity (14, 15). Motolimod (formerly VTX-2337) is a novel, selective, small-molecule TLR8 agonist that mimics viral single-stranded ribonucleic acid (ssRNA), the natural ligand of TLR8 (16). TLR8 in humans is expressed in the endosomal compartment of monocytes and myeloid dendritic cells (mDC) (17). Recent findings demonstrate that TLR8 activation stimulates the release of distinct inflammatory mediators, including Th1-polarizing cytokines and chemokines (18). The combination of cetuximab plus motolimod was safe in a recently completed phase I trial of recurrent/metastatic HNSCC patients (19). We hypothesized that motolimod-stimulated APC that express TLR8, such as monocytes and myeloid-derived suppressor cells (MDSC), could result in a more inflamed tumor site, leading to a stronger cellular immune response to cetuximab by enhancing NK:DC cross talk and induction of adaptive immunity. To validate these findings, we performed a prospective neoadjuvant clinical trial combining motolimod with cetuximab, with the primary endpoint to analyze modulation of immune biomarkers in myeloid and regulatory suppressor T cells (Treg) and the impact on adaptive cellular immunity.

Materials and Methods

Study Design

This was a single-center, open-label, phase Ib “window of opportunity” trial (UPCI #14-002, NCT02124850) approved by the University of Pittsburgh IRB. The trial recruited patients (n=14) with stage II–IVA, previously untreated HNSCC who were candidates for surgical resection of their disease and had no prior history of head and neck cancer. The primary endpoint of this study was to measure quantitative changes in activation and numbers of immune effector cell biomarkers (including NK cells, tumor antigen-specific CTL, reduction in Treg, and TCR repertoire diversity) after the combination of motolimod and cetuximab in the 3–4 weeks prior to scheduled surgery for HNC. Secondary endpoints included measuring modulation of induction of inflammatory markers.

All patients were seen in the Department of Otolaryngology at the University of Pittsburgh Medical Center, and specimens from patients were obtained by informed consent under the IRB approved UPCI protocol 99-069. The study UPCI #14-002 (NCT02124850) was approved by the University of Pittsburgh IRB, and was a single site trial consisting of screening, neoadjuvant treatment, tumor assessment, and surgical removal of tumor. The trial recruited patients (n=14) with stage II–IVA, previously untreated HNSCC who were candidates for surgical resection of their disease and had no prior history of head and neck cancer.

The study was performed in accordance with Good Clinical Practice guidelines and the ethical principles outlined in the Declaration of Helsinki. Approval for the study was obtained from the Institutional Review Board, and all patients provided written informed consent before study enrolment.

Study Treatments and Assessments

Treatment consisted of neoadjuvant doses of subcutaneous motolimod injection (2.5 mg/m^2) and intravenous cetuximab (initial dose of 400 mg/m^2 followed by weekly infusions at 250 mg/m^2) administered once weekly starting on Day 1 for a minimum of 3 weeks and a maximum of 4 weeks (i.e., Days 1, 8, 15, and 22) prior to scheduled surgery, which was to be performed within 2 days of the last dose of motolimod received. Safety monitoring and assessment of AEs was performed at each study visit. AEs were summarized using the Medical Dictionary for Regulatory Activities and graded for severity using NCI CTCAE Version 4.03. Physical exams were conducted prior to the first treatment and on the final treatment day (Day 15 or 22, depending on surgical scheduling). Hematology and chemistry laboratory tests were performed on all patients at screening and prior to the first treatment day; in addition, patients were assessed on day 15 for hypomagnesemia, hypocalcemia and hypokalemia. Tumor imaging assessments were carried out at screening and prior to surgery within 36 hours of the last dose of neoadjuvant therapy. Patients were evaluated for response and progression per the RECIST Version 1.1. End of study and follow-up assessments included hematologic and chemistry laboratory evaluations, in addition to physical examinations and AE monitoring.

Safety and efficacy

Overall, most treatment-related adverse events (TEAEs) were grade 1 or 2. No patients experienced Grade 4 or 5, nor were any new TEAEs observed based on a prior phase Ib trial using this combination (19). The most frequently reported TEAEs were dermatitis acneiform (79%), injection site reaction (79%), and flu-like symptoms (36%) (Table 2). All subjects received the planned resection without delays in performance or extent of surgery.

Collection of peripheral blood lymphocytes (PBL) and tumor infiltrating lymphocytes (TIL)

Tumor and peripheral blood specimens were collected at screening and again at the time of surgery under an IRB-approved tissue banking protocol (UPCI 99-069). Briefly, venous blood from HNSCC patients was drawn into heparinized tubes and centrifuged on Ficoll-Hypaque gradients (GE Healthcare Life Sciences, Piscataway, NJ). PBL were recovered, washed in RPMI-1640 medium (Sigma, St. Louis, MO), and either used immediately for experiments or resuspended in freezing media containing 10% DMSO, transferred to Mr. Frosty containers (Thermo Scientific, Waltham, MA), and stored at −80°C until flow cytometry analysis. For TIL isolation, fresh tumors from HNSCC patients were minced into small pieces manually or using a gentleMACS Dissociator (Miltenyi Biotec, Auburn, CA), then transferred to 70-μm cell strainers and mechanically separated using the plunger of a 5-mL syringe. The cells passing through the cell strainer were collected and subjected to Ficoll-Hypaque gradient centrifugation. After centrifugation, TIL were recovered and stored at −80°C until flow cytometry analysis.

Cell lines and culture

HPV^- HNC cell line JHU029 and HPV^+ cell line UPCI:SCC090 were grown in RPMI-1640 (Sigma) supplemented with 10% fetal bovine serum (Corning Mediatech, Inc.) and 1% penicillin/streptomycin (Invitrogen). JHU029 was a gift from Dr. James Rocco in January of 2006 (Ohio State University). UPCI:SCC090 was isolated from patients treated at the University of Pittsburgh through the explant/culture method, authenticated and validated using STTR profiling and HLA genotyping (20, 21). HNC lines were tested every 6 months and were free of *Mycoplasma* infection.

Antibodies and flow cytometry

The following anti-human mAbs were used for staining: HLA-DR-APC, CD11b-PerCP-Cy5.5, CD163-BV421, CD33-BV421, CD8-APC, PD-1-PE-Cy7, Tim-3-BV421, TIGIT-APC, CD27-Alexa Fluor 700, LAP-BV421, FoxP3-PerCP-Cy5.5 and PD-L1-PE purchased from Biolegend (San Diego, CA); CD11b-PE, CD1c-APC-Cy7, CD141-BV711, CD4-PerCP-Cy5.5, CD56-Alexa Fluor 700, CD3-Alexa Fluor 700, CD19-Alexa Fluor 700, CD16-PE-Cy7 , HLA-A2-APC-H7, CD73-PE, purchased from BD Biosciences (San Jose, CA); CD14-PE-TR purchased from Life Technologies (Carlsbad, CA); CD86-FITC purchased from R&D Systems (Minneapolis, MN); CTLA-4-FITC purchased from Ancell (Bayport, MN); and the PE-labeled HLA-A*0201-EGFR853-861 tetramer obtained from the Tetramer Facility of the National Institute of Allergy and Infectious Disease (Atlanta, GA).

Intracellular staining of FoxP3 was performed as follows: PBL or TIL were stained with surface marker antibodies, fixed with fixation/permeabilization buffer (eBioscience),

washed, and stained for intracellular antigens in 1X permeabilization buffer. Cells were analyzed on an LSR Fortessa (BD) flow cytometer, and data analyzed using Flow Jo (Treestar, Ashland, OR). Dead cells were excluded based on viability dye staining (Zombie Aqua Fixable Viability Dye, Biolegend).

Luminex assays

Peripheral blood of study patients was collected using standard venipuncture techniques prior to neoadjuvant therapy and on the day of surgery. Blood was drawn into heparinized tubes and centrifuged on Ficoll-Paque PLUS gradients. Peripheral blood plasma was recovered from above the PBL layer, aliquoted, frozen, and stored in a dedicated −80°C freezer. Luminex assays of plasma specimens were performed in duplicate using a MILLIPLEX MAP 29-plex human cytokine/chemokine magnetic bead panel for the following analytes: EGF, VEGF, TNF-β, TNF-α, MIP-1β, MIP-1α, MCP-1, IP-10, IL-17, IL-15, IL-13, IL-12 (p70), IL-12 (p40), IL-10, IL-8, IL-7, IL-6, IL-5, IL-4, IL-3, IL-2, IL-1ra, IL-1β, IL-1α, IFN-γ, IFN-α2, GM-CSF, G-CSF, and Eotaxin. Specimens were analyzed by the UPCI IMCPL using the Bio-Plex Multiplex system. Results for each specimen were averaged together and plotted for each analyte. Values that were below the sensitivity of the assay were changed to the lowest detection limit (e.g., values <18 pg/mL changed to 18 pg/mL for G-CSF).

TCR sequencing

DNA was extracted from matched PBL, at both pre-treatment and post-treatment timepoints, using the DNeasy Blood and Tissue kit (Qiagen), and submitted for immunoSEQ profiling (Adaptive Biotechnologies, Seattle, WA) to characterize hs-TCRB chains. Acquired data were analyzed using immunoSEQ Analyzer software.

Statistical analysis

Averages were calculated as means. Two-group comparison was performed using paired Wilcoxon signed rank text in GraphPad Prism (GraphPad, La Jolla, CA). Experimental data with 2 comparison group were analyzed using the paired t test. *$p < 0.05$, **$p < 0.01$.

Results

TLR8 stimulation skews monocytes toward an M1 phenotype

Motolimod is a small molecule TLR8 agonist that can activate monocytes, DC, and NK cells (22) through NF-kB mediated signaling. In order to investigate how TLR8 stimulation affects the activation status of myeloid lineage cells, we cultured HNSCC patient PBL or purified CD14+ monocytes with motolimod (250nM) (22) for 3 days, then analyzed the myeloid cells for phenotypic activation markers. CD14+ cells manifested greatest upregulation of HLA-DR and CD86, indicating a more robust antigen presentation capacity (Figure 1A). Interestingly, these cells also showed a reduction of CD163, which is a scavenger receptor expressed on M2 suppressive macrophages. Moreover, strong upregulation of PD-L1 was also seen, possibly due to activation of monocytes. Thus, we conclude that TLR8 activation can skew myeloid cells to an M1-like phenotype, implying potential value in augmenting antitumor immunity.

Motolimod attenuates suppressive effects of MDSC

Next, we investigated whether the combination of cetuximab and motolimod could modulate M1/M2 macrophage phenotypes. Purified CD14+ monocytes from HNSCC patient PBL were co-cultured with the $EGFR^+$ HNSCC cell lines UPCI:SCC090 and JHU029, incubated in the presence of either IgG1 or cetuximab alone or with motolimod (250nM) for 3 days. Using flow cytometry, we found that addition of motolimod to cetuximab resulted in higher expression of CD86 (an M1 marker) and reduced expression of CD163 (M2 marker). Downregulation of CD16 (evidence of cross-linking by cetuximab-bound HNSCC cells) was further reduced in the presence of motolimod (Figures 1B–1C), indicating stronger ADCC mediated by cetuximab when TLR8 is activated. Notably, expression of macrophage PD-L1 was also increased when incubated with cetuximab plus motolimod, likely due to stronger activation. Based on our finding that motolimod can skew monocytes to a M1 phenotype, we explored whether activation of TLR8 on MDSC could reverse their suppressive activity. Indeed, suppression of T cell proliferation was reduced after co-culture with MDSC under these conditions (Figures 2A–2B). This finding, together with our recent discovery that signaling through CD16 can reverse MDSC suppression of T cell proliferation (23), suggests that the combination of cetuximab and motolimod can contribute to reversing myeloid cell suppression in the TME.

Cetuximab plus motolimod results in increased mDC infiltration into the tumor site

DC play an important role in processing exogenous antigen and inducing adaptive immune responses. mDC are categorized into 2 subsets based on surface CD markers: $CD1c^+$ mDC mediate chemokine production upon activation, whereas CD141+ mDC mainly mediate antigen cross-presentation (24). Based on our *in vitro* findings, we hypothesized that the combination of cetuximab plus motolimod would enhance activation status of innate immune cells. In clinical trial tumor specimens, infiltration by both CD141+ ($p=0.036$) and CD1c+ mDC ($p=0.022$) increased after combination treatment (Figure 3A). The activation marker CD80 was upregulated in both subsets ($p=0.024$ and $p=0.033$, respectively) (Figure 3B), as was surface expression of CD16 ($p=0.027$ and $p=0.017$, respectively) (Figure 3C), indicating a more inflammatory tumor microenvironment with augmented innate immunity promoting mature myeloid APC.

Cetuximab plus motolimod reduces suppressive markers of Treg in the TME and increases inflammatory cytokines in patient plasma

We previously demonstrated that cetuximab monotherapy increases the frequency of intratumoral Treg preferentially in non-responders (25). These Treg cells may suppress NK cell mediated ADCC and CTL, and are associated with poor clinical outcome. In contrast, patients treated with cetuximab in combination with motolimod had reduced phenotypic markers of suppression in Treg (Figure 4A), including lower levels of CTLA-4 ($p=0.002$), CD73 ($p=0.005$) and membrane bound TGF-β ($p=0.012$), resulting in a less suppressive TME. By detecting plasma cytokines using multiplex ELISA (Figure 4B), we found an increase of type 1 inflammatory cytokines such as TNF-α and IP10, which are known to promote antitumor immune responses and prevent angiogenesis.

Cetuximab plus motolimod results in reduced ICR expression on CD8+ TIL

Adaptive antitumor immunity is of significant therapeutic value, and treatments such as anti-PD-1 have yielded promising results in multiple cancer types including HNSCC (26). In order to better assess the antitumor immune response, we compared T cell phenotypic changes in TIL before and after treatment with cetuximab plus motolimod. No significant changes were observed in Treg (p=0.309) or CD4 effector populations (p = 0.766) (Figure 5A). In addition to increased CD8 T cell infiltration (p=0.049), CD8 T cells showed significant upregulation of stimulatory immune receptor CD27 (p=0.025) together with a downregulation of multiple inhibitory immune checkpoint receptors (ICR) such as TIGIT (p=0.047), PD-1 (p=0.041), and CTLA-4 (p=0.053) (Figures 5A–5C; 95% confidence intervals for these markers are summarized in Supplementary Table S1). Since an important feature of T cell exhaustion is expression of multiple inhibitory receptors, our results suggest an enhanced CD8+ T cell activation, indicated by reduced expression of ICR and upregulated stimulatory receptors following therapy with cetuximab plus motolimod.

Cetuximab plus motolimod increases circulating tumor antigen-specific T cells and phenotypic activation

In the setting of stronger functionality of tumor infiltrating CD8 T cells, we investigated whether the enhanced immune response was tumor antigen-specific. TCR sequencing in peripheral blood showed that T cell productive clonality was significantly increased after treatment (p=0.0012) (Figure 6B). These data indicate amplified T cell clones are induced in patients receiving cetuximab plus motolimod, potentially mediating an antigen-specific antitumor immune response. Corroborating this finding, we used fluorescent multimers to observe an expansion of EGFR-specific CD8+ T cells in peripheral blood in HLA-A2+ patients (n=5) after treatment with cetuximab plus motolimod (p=0.048) (Figure 6A). These results suggest expansion of circulating antigen-specific CD8 T cells after treatment with cetuximab plus motolimod.

Discussion

Building on a cetuximab monotherapy trial in which poor clinical response was associated with induction of CTLA4+ Treg (9), we added a pro-inflammatory TLR8 agonist to skew suppressive myeloid cells and effector T lymphocytes toward a more activated and functionally antitumor phenotype. In the present study, we hypothesized that generation of inflammation using motolimod might enhance type 1 cytotoxic T lymphocyte responses and NK:DC priming. Selective TLR8 expression on suppressive myeloid cells and MDSC provided the basis for targeting these APC to promote the immune stimulating effects mediated by cetuximab (5, 7, 27).

In this phase Ib clinical trial, active modulation in the tumor microenvironment was observed using TLR8 stimulation to enhance cetuximab-mediated cellular immune modulation over 4 weeks. A longer window may be needed for tumor efficacy analysis to correlate tumor response and survival with these biomarker changes. However, our findings to date provide evidence that cetuximab plus motolimod enhances modulation of host immunity, which was previously observed with cetuximab alone (25). Beneficial effects

were seen in both innate and adaptive immunity. Larger studies need to be performed by assessing clinical efficacy of adding additional immune checkpoint receptor modulation.

The anti-EGFR antibody cetuximab binds to EGFR expressed on tumor cells and blocks downstream signaling to interrupt tumor cell growth (28). However, despite relatively universal EGFR expression on HNSCC cells, single agent cetuximab results in only a 15–20% response rate. In this context, we considered that cetuximab can also mediate ADCC for a more specific tumor cell killing, triggering a cascade of adaptive immune cell stimulation through NK:DC priming. Our previous studies using specimens from a cetuximab monotherapy neoadjuvant clinical trial by Jie et al (25) and Li et al (23) suggest that cetuximab skews monocytes toward a beneficial macrophage phenotype, but also resulted in more CTLA-4+ Treg infiltration in the TME, which was correlated with a poor prognosis of patients. Moreover, Li et al also showed that during cetuximab monotherapy treatment, increased circulating MDSC were observed in clinical non-responders. Thus, we aimed to evaluate combinatorial therapy adding a pro-inflammatory TLR8 stimulus, due to its expression on monocytes and myeloid DC. We hypothesized that this combination may generate beneficial inflammatory signals in the microenvironment, skewing suppressive populations such as macrophages and MDSC toward an antitumor phenotype. Functionally, this might result in lower Treg, which has been correlated with poor clinical outcome in cetuximab monotherapy treated HNSCC patients.

MDSC are known to be induced by multiple tumor-derived soluble factors. Upon activation, these cells can mediate suppression of both innate and adaptive immune responses in the TME (29–31). Secretion of IL-10 and TGF-β by MDSC can skew tumor-associated macrophages toward an M2-like phenotype, and also suppress NK cell functions (32, 33). Furthermore, MDSC can also suppress T cell proliferation and activation, as well as inducing Treg, promoting tumor cell evasion from immune surveillance (34–36). In order to induce a robust antitumor immune response, reversing the suppressive microenvironment is essential. Modulation of immune cells using mAbs are becoming an important regimen of cancer therapy, and late stage cancer patients remains highly sensitive to TLR8 agonist motolimod as reported by Gregory and colleagues (37). By conducting *in vitro* incubation of chemokine-induced MDSC with motolimod we found that addition of motolimod reversed suppression on T cell proliferation by MDSC. Our previous findings by Stephenson et al revealed that TLR8 stimulation enhances cetuximab-mediated NK cell lysis of HNSCC cells (22); we then wished to find out if cetuximab plus motolimod could result in better antitumor immunity.

Using a novel neoadjuvant trial, our findings suggest that cetuximab plus TLR8 stimulation using motolimod induces inflammatory changes in the TME and peripheral blood. Greater APC frequency and activation status were seen, corresponding to higher frequency of CD8+ T cells and reduced MDSC infiltration in TIL. Treg suppressive mediators were reduced after the addition of motolimod, overcoming a negative prognostic biomarker (Treg induction) observed previously with cetuximab monotherapy (25). Furthermore, enrichment of EGFR antigen-specific CD8 T cells in peripheral circulation and increased clonality of T cells in peripheral blood suggest that priming of a stronger cellular adaptive immune response is a consequence of the inflammatory modulation. Importantly, Srivastava et al

previously reported that cetuximab monotherapy resulted in increased circulating EGFR-specific CD8+ T cells (5). Further study is needed to confirm whether motolimod has an additive effect in inducing tumor antigen-specific CD8+ T cells. Upregulated costimulatory CD27 and downregulated expression of inhibitory TIGIT receptor suggests that CD8+ T cells in the microenvironment might be more functional and less exhausted. Interestingly, increases of IL-10 and IL-1RA were also detected in peripheral circulation (Supplementary Figure S1A) despite the increase of IP-10 and TNFα, indicative that although a skew toward suppressive TME is observed, it is important to further overcome the anti-inflammatory signals for better antitumor immune response. We also observed a decrease of eotaxin in the peripheral circulation (Supplementary Figure S1B), which is an eosinophil chemotactic protein, the role of which should be further established in future study. Our findings also suggest that the addition of a PD-1 inhibitor to the combination of cetuximab and motolimod would further augment the antitumor response. As the PD-1:PD-L1 pathway is enriched in HNSCC, and anti-PD-1 treatment is shown to be effective in 15–20% of patients, it is likely that addition of PD-1 blockade to the combination of cetuximab and motolimod will further augment the antitumor immune response.

Supplementary Material

Refer to Web version on PubMed Central for supplementary material.

Acknowledgments

Financial support: (Robert L. Ferris) National Institute of Health grants R01 CA206517, DE019727, P50 CA097190, T32 CA060397, and the University of Pittsburgh Cancer Institute award P30 CA047904.

Supported by NIH grant R01 CA206517, DE019727, P50 CA097190, T32 CA060397, and the University of Pittsburgh Cancer Institute award P30 CA047904. This project used the UPCI Flow Cytometry Facility that is supported in part by award P30 CA047904. Gulidanna Shayan were supported by the China Scholarship Council.

References

1. Pulte D, Brenner H. Changes in survival in head and neck cancers in the late 20th and early 21st century: a period analysis. Oncologist. 2010; 15:994–1001. [PubMed: 20798198]
2. Rischin D, Ferris RL, Le QT. Overview of Advances in Head and Neck Cancer. J Clin Oncol. 2015; 33:3225–3226. [PubMed: 26351331]
3. Leemans CR, Braakhuis BJ, Brakenhoff RH. The molecular biology of head and neck cancer. Nat Rev Cancer. 2011; 11:9–22. [PubMed: 21160525]
4. Shin DM, Donato NJ, Perez-Soler R, Shin HJ, Wu JY, Zhang P, Lawhorn K, Khuri FR, Glisson BS, Myers J, et al. Epidermal growth factor receptor-targeted therapy with C225 and cisplatin in patients with head and neck cancer. Clin Cancer Res. 2001; 7:1204–1213. [PubMed: 11350885]
5. Srivastava RM, Lee SC, Andrade Filho PA, Lord CA, Jie HB, Davidson HC, Lopez-Albaitero A, Gibson SP, Gooding WE, Ferrone S, et al. Cetuximab-activated natural killer and dendritic cells collaborate to trigger tumor antigen-specific T-cell immunity in head and neck cancer patients. Clin Cancer Res. 2013; 19:1858–1872. [PubMed: 23444227]
6. Lopez-Albaitero A, Lee SC, Morgan S, Grandis JR, Gooding WE, Ferrone S, Ferris RL. Role of polymorphic Fc gamma receptor IIIa and EGFR expression level in cetuximab mediated, NK cell dependent in vitro cytotoxicity of head and neck squamous cell carcinoma cells. Cancer Immunol Immunother. 2009; 58:1853–1864. [PubMed: 19319529]

7. Lee SC, Srivastava RM, Lopez-Albaitero A, Ferrone S, Ferris RL. Natural killer (NK): dendritic cell (DC) cross talk induced by therapeutic monoclonal antibody triggers tumor antigen-specific T cell immunity. Immunol Res. 2011; 50:248–254. [PubMed: 21717064]
8. Ferris RL, Jaffee EM, Ferrone S. Tumor antigen-targeted, monoclonal antibody-based immunotherapy: clinical response, cellular immunity, and immunoescape. J Clin Oncol. 2010; 28:4390–4399. [PubMed: 20697078]
9. Jie HB, Schuler PJ, Lee SC, Srivastava RM, Argiris A, Ferrone S, Whiteside TL, Ferris RL. CTLA-4(+) Regulatory T Cells Increased in Cetuximab-Treated Head and Neck Cancer Patients Suppress NK Cell Cytotoxicity and Correlate with Poor Prognosis. Cancer Res. 2015; 75:2200–2210. [PubMed: 25832655]
10. Dougan M, Dranoff G. Immune therapy for cancer. Annu Rev Immunol. 2009; 27:83–117. [PubMed: 19007331]
11. Seya T, Begum NA, Nomura M, Tsuji S, Matsumoto M, Hayashi A, Azuma I, Toyoshima K. Innate immune therapy for cancer. Screen for molecules capable of activating the innate immune system. Adv Exp Med Biol. 2000; 465:229–237. [PubMed: 10810630]
12. Diefenbach A, Raulet DH. The innate immune response to tumors and its role in the induction of T-cell immunity. Immunol Rev. 2002; 188:9–21. [PubMed: 12445277]
13. Gajewski TF, Schreiber H, Fu YX. Innate and adaptive immune cells in the tumor microenvironment. Nat Immunol. 2013; 14:1014–1022. [PubMed: 24048123]
14. Cervantes JL, Weinerman B, Basole C, Salazar JC. TLR8: the forgotten relative revindicated. Cell Mol Immunol. 2012; 9:434–438. [PubMed: 23085951]
15. Takeda K, Akira S. Roles of Toll-like receptors in innate immune responses. Genes Cells. 2001; 6:733–742. [PubMed: 11554921]
16. Lu H, Dietsch GN, Matthews MA, Yang Y, Ghanekar S, Inokuma M, Suni M, Maino VC, Henderson KE, Howbert JJ, et al. VTX-2337 is a novel TLR8 agonist that activates NK cells and augments ADCC. Clin Cancer Res. 2012; 18:499–509. [PubMed: 22128302]
17. Takeda K, Akira S. Toll-like receptors in innate immunity. Int Immunol. 2005; 17:1–14. [PubMed: 15585605]
18. Gosu V, Basith S, Kwon OP, Choi S. Therapeutic applications of nucleic acids and their analogues in Toll-like receptor signaling. Molecules. 2012; 17:13503–13529. [PubMed: 23151919]
19. Chow LQ, Morishima C, Eaton KD, Baik CS, Goulart BH, Anderson LN, Manjarrez KL, Dietsch GN, Bryan JK, Hershberg RM, et al. Phase Ib Trial of the Toll-like Receptor 8 Agonist, Motolimod (VTX-2337), Combined with Cetuximab in Patients with Recurrent or Metastatic SCCHN. Clin Cancer Res. 2016
20. Zhao M, Sano D, Pickering CR, Jasser SA, Henderson YC, Clayman GL, Sturgis EM, Ow TJ, Lotan R, Carey TE, et al. Assembly and initial characterization of a panel of 85 genomically validated cell lines from diverse head and neck tumor sites. Clin Cancer Res. 2011; 17:7248–7264. [PubMed: 21868764]
21. Heo DS, Snyderman C, Gollin SM, Pan S, Walker E, Deka R, Barnes EL, Johnson JT, Herberman RB, Whiteside TL. Biology, cytogenetics, and sensitivity to immunological effector cells of new head and neck squamous cell carcinoma lines. Cancer Res. 1989; 49:5167–5175. [PubMed: 2766286]
22. Stephenson RM, Lim CM, Matthews M, Dietsch G, Hershberg R, Ferris RL. TLR8 stimulation enhances cetuximab-mediated natural killer cell lysis of head and neck cancer cells and dendritic cell cross-priming of EGFR-specific CD8+ T cells. Cancer Immunol Immunother. 2013; 62:1347–1357. [PubMed: 23685782]
23. Li J, Srivastava RM, Ettyreddy A, Ferris RL. Cetuximab ameliorates suppressive phenotypes of myeloid antigen presenting cells in head and neck cancer patients. J Immunother Cancer. 2015; 3:54. [PubMed: 26579227]
24. Ziegler-Heitbrock L, Ancuta P, Crowe S, Dalod M, Grau V, Hart DN, Leenen PJ, Liu YJ, MacPherson G, Randolph GJ, et al. Nomenclature of monocytes and dendritic cells in blood. Blood. 2010; 116:e74–80. [PubMed: 20628149]

25. Jie HB, Schuler PJ, Lee SC, Srivastava RM, Argiris A, Ferrone S, Whiteside TL, Ferris RL. CTLA-4+ Regulatory T Cells are Increased in Cetuximab Treated Head and Neck Cancer Patients, Suppress NK Cell Cytotoxicity and Correlate with Poor Prognosis. Cancer Res. 2015

26. Ferris RL, Blumenschein G Jr, Fayette J, Guigay J, Colevas AD, Licitra L, Harrington K, Kasper S, Vokes EE, Even C, et al. Nivolumab for Recurrent Squamous-Cell Carcinoma of the Head and Neck. N Engl J Med. 2016; 375:1856–1867. [PubMed: 27718784]

27. Srivastava RM, Trivedi S, Concha-Benavente F, Gibson SP, Reeder C, Ferrone S, Ferris RL. CD137 stimulation enhances cetuximab induced natural killer (NK): dendritic cell (DC) priming of anti-tumor T cell immunity in head and neck cancer patients. Clin Cancer Res. 2016

28. Lopez-Albaitero A, Ferris RL. Immune activation by epidermal growth factor receptor specific monoclonal antibody therapy for head and neck cancer. Arch Otolaryngol Head Neck Surg. 2007; 133:1277–1281. [PubMed: 18086972]

29. Gabrilovich DI, Ostrand-Rosenberg S, Bronte V. Coordinated regulation of myeloid cells by tumours. Nat Rev Immunol. 2012; 12:253–268. [PubMed: 22437938]

30. Ostrand-Rosenberg S. Myeloid-derived suppressor cells: more mechanisms for inhibiting antitumor immunity. Cancer Immunol Immunother. 2010; 59:1593–1600. [PubMed: 20414655]

31. Ochando JC, Chen SH. Myeloid-derived suppressor cells in transplantation and cancer. Immunol Res. 2012; 54:275–285. [PubMed: 22535241]

32. Sinha P, Clements VK, Bunt SK, Albelda SM, Ostrand-Rosenberg S. Cross-talk between myeloid-derived suppressor cells and macrophages subverts tumor immunity toward a type 2 response. J Immunol. 2007; 179:977–983. [PubMed: 17617589]

33. Marcoe JP, Lim JR, Schaubert KL, Fodil-Cornu N, Matka M, McCubbrey AL, Farr AR, Vidal SM, Laouar Y. TGF-beta is responsible for NK cell immaturity during ontogeny and increased susceptibility to infection during mouse infancy. Nat Immunol. 2012; 13:843–850. [PubMed: 22863752]

34. Srivastava MK, Sinha P, Clements VK, Rodriguez P, Ostrand-Rosenberg S. Myeloid-derived suppressor cells inhibit T-cell activation by depleting cystine and cysteine. Cancer Res. 2010; 70:68–77. [PubMed: 20028852]

35. Hoechst B, Ormandy LA, Ballmaier M, Lehner F, Kruger C, Manns MP, Greten TF, Korangy F. A new population of myeloid-derived suppressor cells in hepatocellular carcinoma patients induces CD4(+)CD25(+)Foxp3(+) T cells. Gastroenterology. 2008; 135:234–243. [PubMed: 18485901]

36. Serafini P, Mgebroff S, Noonan K, Borrello I. Myeloid-derived suppressor cells promote cross-tolerance in B-cell lymphoma by expanding regulatory T cells. Cancer Res. 2008; 68:5439–5449. [PubMed: 18593947]

37. Dietsch GN, Randall TD, Gottardo R, Northfelt DW, Ramanathan RK, Cohen PA, Manjarrez KL, Newkirk M, Bryan JK, Hershberg RM. Late-Stage Cancer Patients Remain Highly Responsive to Immune Activation by the Selective TLR8 Agonist Motolimod (VTX-2337). Clin Cancer Res. 2015; 21:5445–5452. [PubMed: 26152744]

Translational relevance

HNSCC patients only show a response rate of 15–20% to anti-EGFR treatment despite the nearly universal overexpression of EGFR, and the suppressive tumor microenvironment may contribute to this low response rate. Harnessing the immune stimulating effect of the selective TLR8 agonist motolimod, we performed a neoadjuvant trial of motolimod plus cetuximab in resectable HNSCC patients, including extensive immune profiling of tumor infiltrating lymphocytes (TIL). Indeed, motolimod skewed monocytes toward a more M1-phenotype. Furthermore, by analyzing immune biomarker changes in patient TIL and PBL from a phase Ib clinical trial, cetuximab plus motolimod treatment resulted in a more immunogenic TME and reversed suppressive signals mediated by myeloid cells and immune checkpoint receptors. More antigen-specific T cells were detected using TCR sequencing and flow cytometric tetramer staining, indicative of enhanced T cell priming. Our work provides insight into potential immunomodulation in combination with therapeutic mAb treatment.

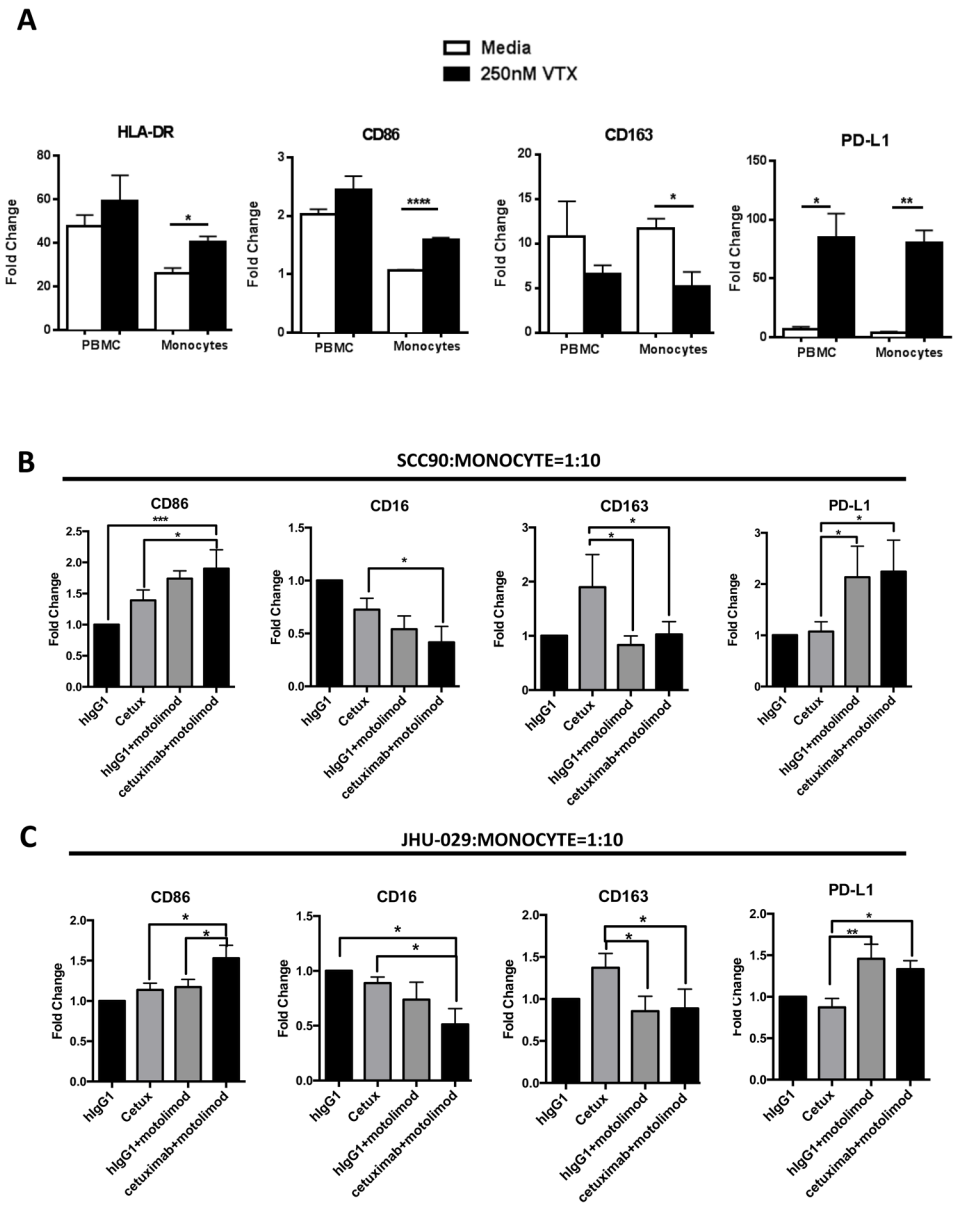

Figure 1.

(A) HNSCC patient PBL and monocytes alone were treated with 250 nM motolimod for 18 hr. Summary data show induction of M1-type macrophage associated surface molecules HLA-DR and CD86, M2-type associated markers CD163, and immune suppressive marker PD-L1; MFI are normalized to the isotype control of each marker (n=5). (B) Purified CD14+ monocytes from HNSCC patients were isolated and co-cultured with UPCI:SCC090 cells or (C) JHU029 cells at a 10:1 ratio. Cetuximab (10ug/ml) and motolimod (250nM) were then added, with hIgG1 used as a control for cetuximab. Summary data show expression changes of CD86, CD16, CD163 and PD-L1, where fold change indicates MFI normalized to IgG1 isotype control treatment group (n=5). Significance was calculated with repeated measures one-way ANOVA. *p<0.05; **p<0.01.

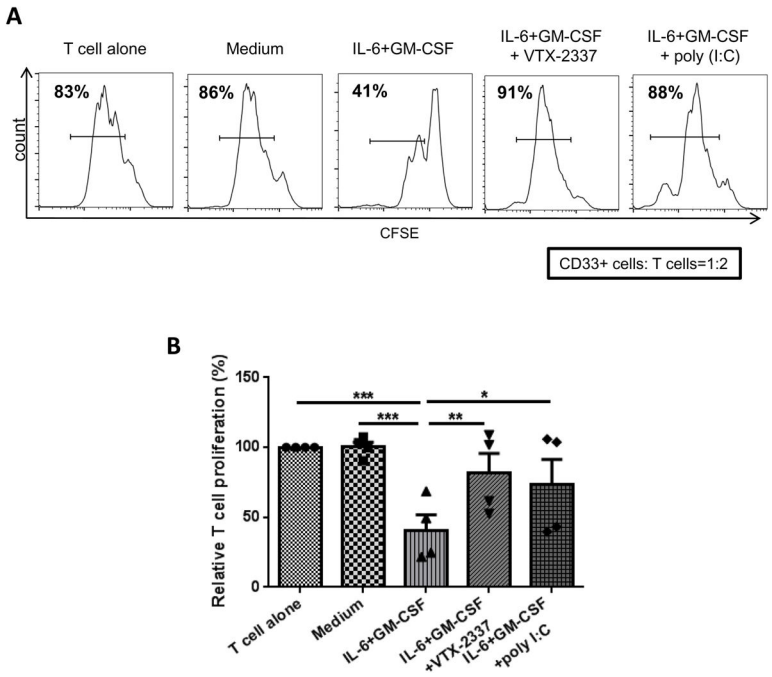

Figure 2.

HNSCC patient monocytes were cultured in T-75 flasks at $5x10^5$ cells/mL in complete medium with or without 10ng/mL GM-CSF and IL-6 for 7 days in the presence of motolimod or poly I:C. Medium and cytokines were refreshed every 2–3 d. Cells were then harvested and CD33+ cells purified by FACS sorting. Autologous T cells were isolated, labeled with CFSE and seeded in 96-well plates at 10^5/well. CD33+ cells from the above cultures were added to these cells at a 1:2 ratio. T cell stimulation was provided by anti-CD3/CD28 stimulation beads (bead:T cell = 1:1). Proliferation of T cells was analyzed by flow cytometry after 3 days. (A) Representative flow plot and (B) summary data are shown. Significance was calculated using one-way ANOVA followed by Tukey's test, *$p<0.05$; **$p<0.01$.

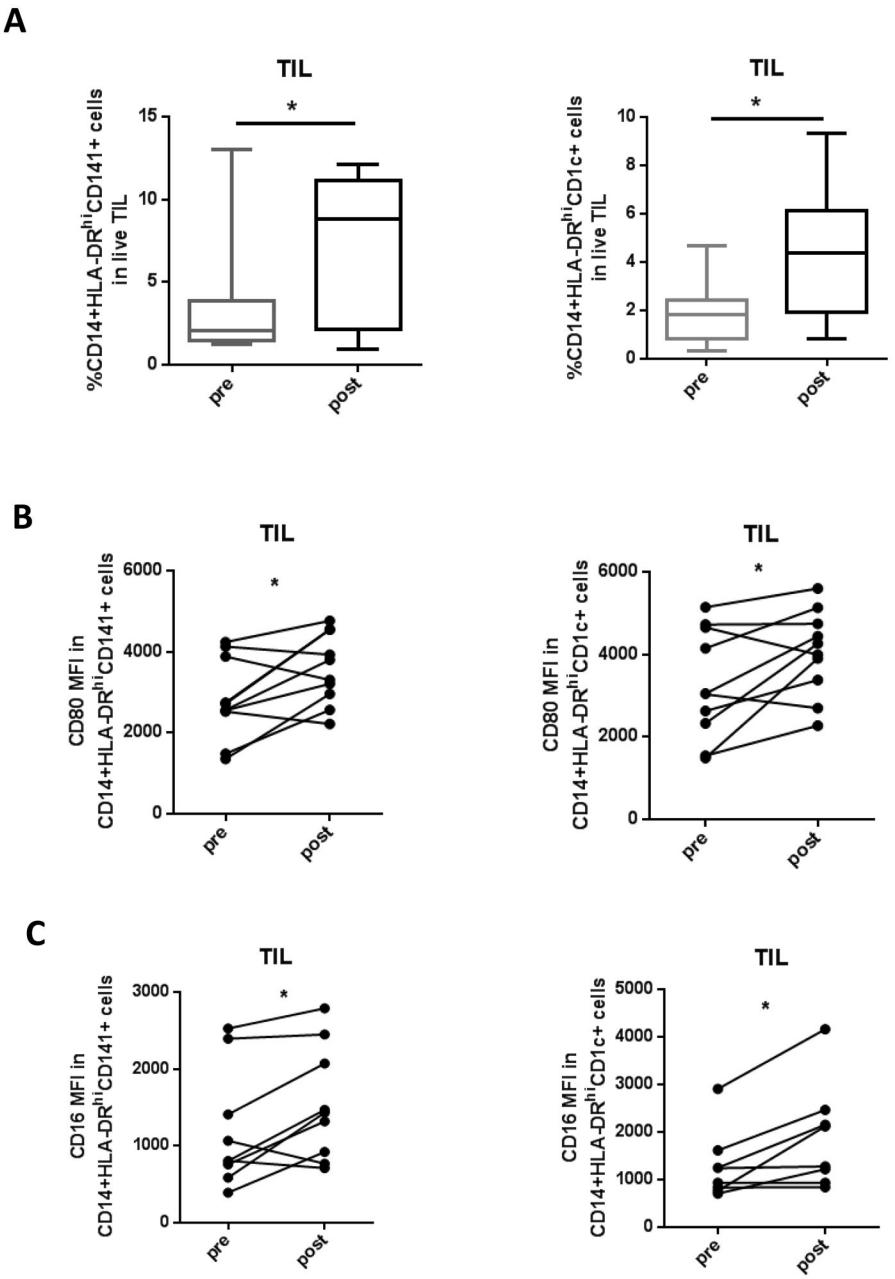

Figure 3.

Clinical trial patient TIL were collected pre- and post-treatment regimen and monocytic populations analyzed using flow cytometry. (A) Summary data of percentage of CD14+HLA-DR^{hi}CD68+ and CD14+CD33+HLA-DR^{low} monocytes pre- and post-treatment are shown (n=9). (B) Summary data of CD80 and CD16 expression pre- and post-treatment on CD141+ DC and (C) CD1c+ DC are shown (n= 9). Significance was calculated with paired t test, *$p<0.05$.

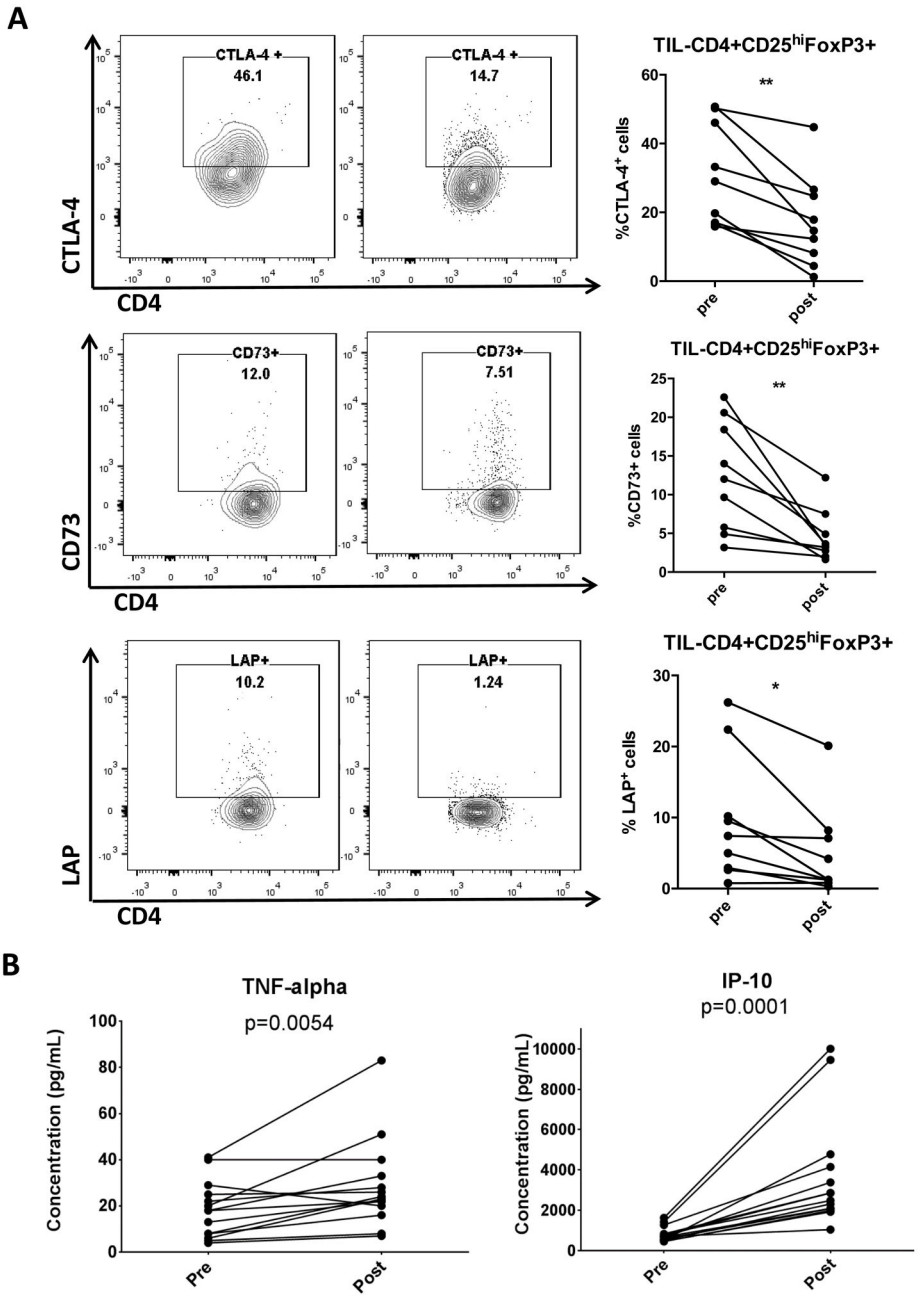

Figure 4.

(A) Clinical trial patient TIL were collected pre- and post-treatment regimen and analyzed for suppressive markers using flow cytometry. Representative flow plots and summary data of percentage of CTLA-4, CD73 and LAP on CD4+CD25^{hi}Foxp3+ Treg are shown (n=9). (B) Luminex analysis of clinical trial patient plasma specimens was performed in duplicate using a MILLIPLEX MAP 29-plex human cytokine/chemokine bead panel. Data show plasma concentrations of TNFα and IP-10 (n=14). Significance was calculated with paired t test, *p<0.05; **p<0.01.

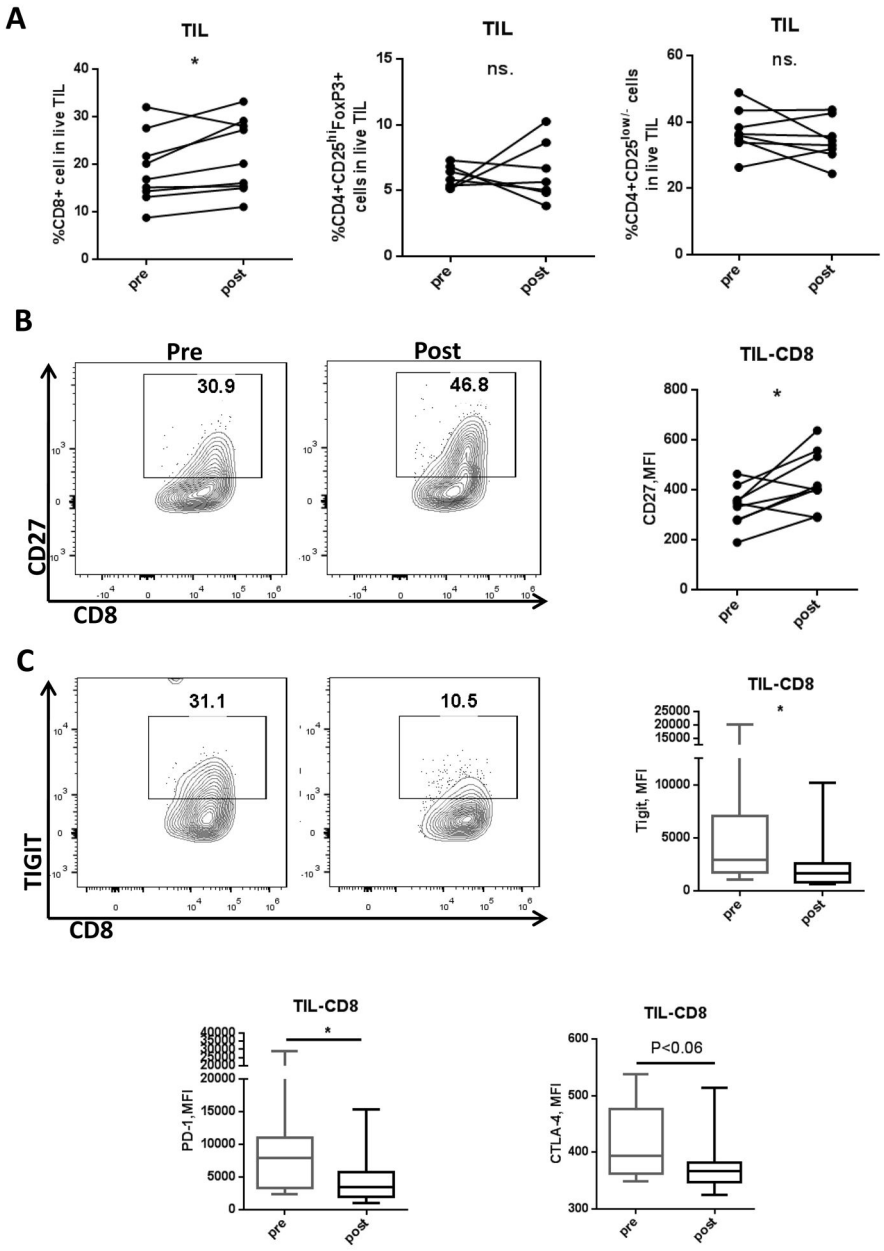

Figure 5.

Clinical trial patient TIL were collected both pre- and post-treatment regimen and lymphocyte populations analyzed using flow cytometry. (A) Summary data showing percentage of CD8, CD4 effector, and Treg population in TIL (n=8 or 9). (B) Representative flow plot and summary data showing MFI changes of CD27 pre- and post-treatment in CD8+ TIL (n=9). (C) Representative flow plot showing expression of TIGIT and summary data showing TIGIT, PD-1, CTLA-4 MFI changes pre- and post-treatment in CD8+ TIL (n=9). Significance was calculated by paired t test, *p<0.05; **p<0.01.

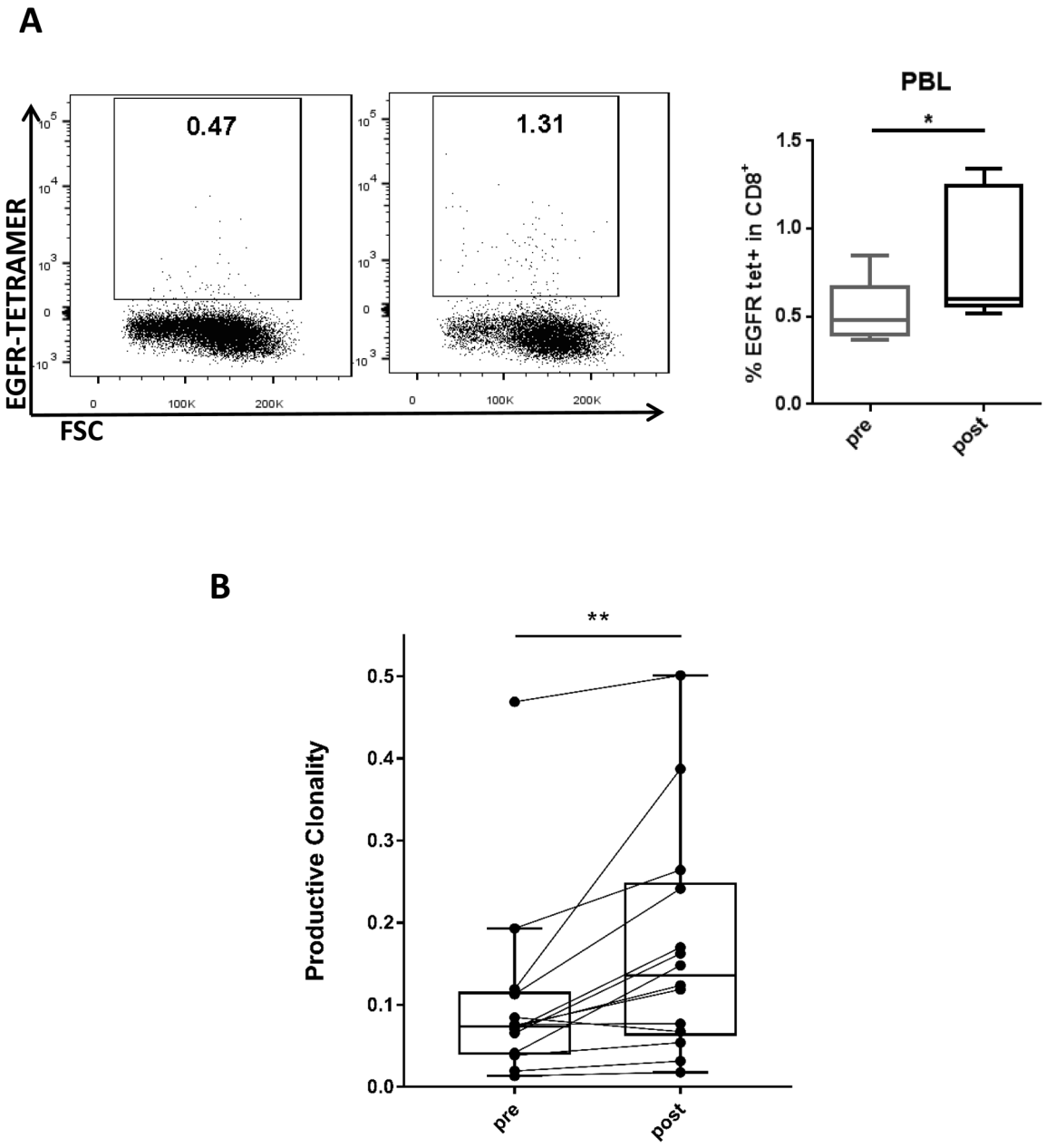

Figure 6.

(A) Representative flow plot and summary data showing percentage of EGFR tetramer+ CD8 T cells in PBL of HLA-A2+ patients pre- and post-treatment (n=5). (B) DNA from clinical trial patient PBL were analyzed using TCR sequencing (Adaptive, Seattle, WA). Data show productive clonality pre- and post-treatment (p = 0.0012, Wilcoxon signed rank test) (n=14). (C) Summary data showing percentage of PD-1^{hi} and PD-1^{int} populations within EGFR tetramer+ cells (n=5). Significance was calculated using the paired t test, *p<0.05; **p<0.01.

Table 1

Characteristics at Baseline

	(n=14)
Age, years; median (range)	61 (43–75)
Sex, n (%)	
Female	5 (36)
Male	9 (64)
Clinical Stage, n (%)	
Stage III	3 (21)
Stage IVA	11 (79)
T Stage, n (%)	
T1	1 (7)
T2	0 (0)
T3	4 (29)
T4	9 (64)
N Stage, n (%)	
N0	5 (36)
N1	1 (7)
N2A	1 (7)
N2B	4 (29)
N2C	3 (21)
Tumor Site, n (%)	
Oral Cavity	10 (71)
Oropharynx	1 (7)
Hypopharynx	1 (7)
Larynx	2 (14)

Table 2

Treatment-Related Adverse Events Occurring in at Least 20% of Patients

Event	(n=14) # of patients (%)
Injection site reaction	11 (79)
Rash acneiform	11 (79)
Flu-like symptoms	5 (36)
Fatigue	3 (21)
Diarrhea	3 (21)
Malaise	2 (14)
Fever	2 (14)
Infusion reaction	2 (14)
Headache	2 (14)